Memoirs of the Faculty of Engineering, Kyushu University, Vol.72, No.2, June 2012

An Approach from Earthquake-Induced Landslides Identification to Numerical Simulation of Debris Flow

by

Yange LI[*], Guangqi CHEN[**], Chuan TANG[***], Lu ZHENG[†] and Yingbin ZHANG[*]

(Received May 7, 2012)

Abstract

On August 14, 2010, an intense and prolonged rainfall triggered debris flow in Hongchun Gully, Yingxiu Town, the epicenter of Wenchuan earthquake. The event transported huge sediment material to the watercourse of the Minjiang River and formed a natural dam, resulting in flash flood in the new reconstruction Yingxiu Town. In order to predict the run out distance and extent of the hazard area of such kind of debris flows, we develop an approach from earthquake-induced landslides investigation to numerical simulation of debris flow in this study. At first, we determined the loose deposits by aerial photography identification and field investigation. Six large scale landslides were found in Hongchun Gully by using the object-oriented analysis remote sensing technique. And then, a two-dimensional numerical model was used to simulate the transport process of debris flow. Raster grid network of digital elevation model generated from GIS was used for the finite difference mesh. Results from the numerical simulation showed a good agreement with actual movement and deposition distribution of Hongchun Gully debris flow.

Keywords: Aerial photography identification, Object-oriented analysis, Debris flow, Two-dimensional numerical model, GIS

1. Introduction

The 12 May 2008 Wenchuan earthquake, with the characteristics of high magnitude (Ms. 8.0), shallow hypocenter (the depth of the hypocenter was less than 20 km), long fracture zone (approximately 300 km), great rupture (the largest rupture was about 7 m), large energy release (three times of 1976 Tangshan earthquake) and long duration (the main shock duration was about

[*] Graduate Student, Department of Civil and Structural Engineering
[**] Professor, Faculty of Arts and Science & Department of Civil Engineering, Graduate School of Engineering
[***] Professor, Department of State Key Laboratory of Geo-Hazard Prevention, Chengdu University of Technology, China
[†] Post-doctoral research fellow, Department of Civil and Structural Engineering

120 s) [1], has triggered as many as 56,000 landslides of various types in steep mountainous terrain in Sichuan Province, China, throughout an area of about 41,750 km^2 [2]. What is more serious is that the strong earthquake not only intensively disturbs ground strata but also can increase post-seismic slope in-stability for a long period of time [3,4]. For example, on September 24, 2008, a heavy rainfall resulted in 72 debris flows in Beichuan County, and led to 42 people dead as well as great damages to roads and relocation area for people suffered from the earthquake. A huge debris flow generated in Zhouqu City on August 8, 2010 caused 1434 people dead and 331 be missing. This destructive debris flow was induced by a serve rainstorm and destroyed more than 5500 houses along its flow path. Besides, a severe rainstorm gave rise to 21 debris flows around Yingxiu Town on August 14, 2010. Out of the 21 debris flow, the severest one occurred in Hongchun Gully, Yingxiu Town. It carried large amount of sediment to Minjiang River and formed a natural debris dam of 10 m height, 100 m in length and 150 m in width, which then changed the channel of Minjiang River and caused a flood in the newly reconstructed Yingxiu Town (**Fig.1**). An estimation of the food water depth is at 2.5-3.0 m and the flood duration lasted for 7 days, which caused 13 people dead and 59 being listed as missing. Approximately 8000 residents had no choice but to leave their homes.

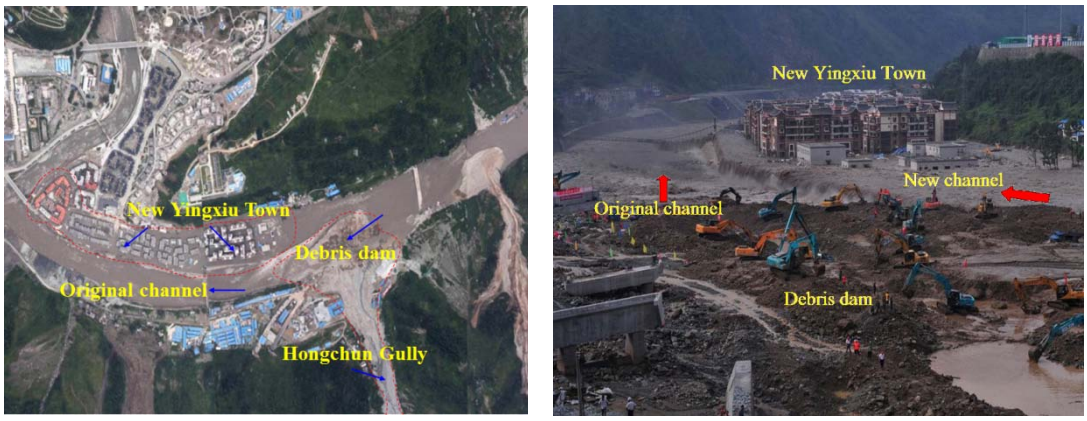

(a) Aerial photograph showing the blocked Minjiang River

(b) New Yingxiu Town in flood

Fig. 1 The flooded new Yingxiu Town triggered by the Hongchun Gully debris flow.

All the events and previous researches showed strong earthquakes play a major role in contributing to the accumulation of sediment deposits on hillslope and in channels. Debris flow is triggered by a combination of three essential factors: sufficient available loose material, surface runoff, and steepness of the drainage channels on the slopes [5]. Therefore, the sediment supply is vital to debris flow hazard analysis. Traditionally, there is only one source area for one debris flow, and the sediment material can be easily derived from field investigation. However, in areas where large amount of landslides triggered by strong earthquake, such as Sichuan Provence, debris flow usually has more than one source area. Therefore an automatic approach is very important to discover the sediment condition. The newly developed remote sensing technology can identify landslides rapid, and quick detection of landslides is very helpful for relief and rescue works after disasters. Many automatic techniques have been developed for landslide recognition. For example, Nichol and Wong [6] aimed to differentiate landslides from spectral similar features like bare ground by using automated change detection. Some emerging theses attempted to use more automated extraction techniques, utilizing band ratios [7], image difference [8], unsupervised [9] and supervised classification [10], to reduce the level of manual interpretation. These theses provide reasonable accuracy up to 80%. The accuracy is usually suffering from mis-classification of landslides and

bare ground. Moreover, since geomorphic process cannot be represented only with pixel digital number (DN) values, all the automatic pixel-based methods mentioned above are ill-suited to detect landslides and give 'salt and pepper' noises in output. Therefore, object-oriented method, which integrates the spectral, spatial, texture and context together to group the homogeneous pixels, is better to detect landslides automatically than pixel-based methods [11,12].

For debris flow analysis, great efforts have been carried out before in order to understand the mechanism of debris flow [13]. Also, some studies focus on field observations as well as laboratory experiments aiming at characterizing the mechanism of debris flow [14]. Practically, some researchers attempt to develop prediction tools to estimate the potential hazard areas or defining triggering threshold of debris flows [15].

In this study, in order to predict potential debris arising from the deposits of earthquake-induced landslides, we develop an approach from earthquake-induced landslides investigation to numerical simulation of the debris flow. At first, we determined the initial sediment deposits by aerial photography identification and field investigation. Six large scale landslides in the Hongchun Gully were recognized by using object-oriented analysis technique and they were thought as the main loose material of debris flow, the volume was estimated by the scale of landslides and field investigation. And then, we used a two-dimensional numerical model to simulate the transport process of debris flow. In the model, debris and water mixture was assumed to be a uniform continuous, incompressible and unsteady Newtonian turbulence fluid. Raster grid network of digital elevation model generated from GIS was used for the finite difference mesh. The model is expected to simulate the typical debris flow case in Hongchun Gully. A real propagation process of the debris flow, the potential inundation area and the maximum flow depth have been estimated from the simulation, which showed a good agreement with the field investigation result.

2. Study Area and Data Source

The Hongchun Gully (**Fig.2**) is situated on the left bank of Minjiang River and in the northeast of Wenchuan County, Sichuan Province, China. The gully-mouth is located at 31°04'01"N and 103°29'33"E. The study area is situated in the transitional mountainous belt between Sichuan Basin and Western Sichuan Plateau, with a catchment area of approximately 5.35 km^2 and a channel length of 3.55 km. The upslope elevation of the gully is more than 1700 m and the gully mouth is at 880 m. The highest part of the debris flow source area is at 2168 m. The terrain on each side of the gully is very steep and slope gradient reaches a maximum of about 70°, with a mean value of 35°.

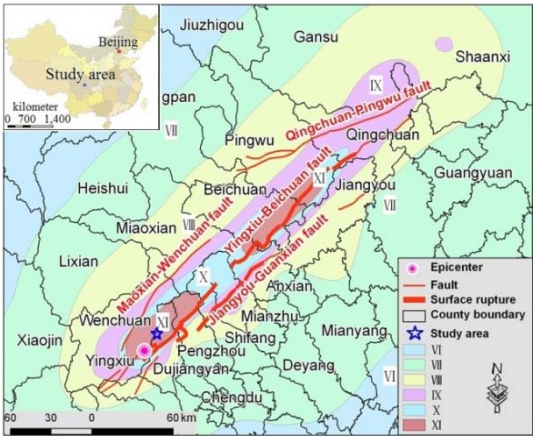

Fig. 2 Location of the study area with seismic intensity map of Wenchuan earthquake, VI, VII ... represent the earthquake magnitude contours.

The study area is underlain by Granitic rocks, Sinian pyroclastic rocks, Carboniferous limestones, and Triassic sandstones. All bedrock is deeply fractured and highly weathered, and covered with a layer of weathered material. Joints developed in the slope surface, which combined with active faulting, produces many potential failure surfaces in the rock slopes. The main geological structure and the strike of the rock strata in the study area show a NE-SW orientation. The Yingxiu-Beichuan fault, which is the seismogenic fault of Wenchuan earthquake, has cross the southeastern part of the study area. It is a northwest-dipping thrust fault with dip angles of 60-70° with a mean thrust offset of 3-4 m and a mean right lateral slip offset of 1-2 m near Yingxiu.

Hongchun Gully is situated in the typical humid subtropical, monsoon climate zone. The annual average precipitation over a period of 30 years is 1253 mm, with the highest recorded annual precipitation of 1688 mm in 1964. On average, 70% of the annual precipitation is largely concentrated from June to September. The maximum recorded rainfall intensity was 269.8 mm/day in 1964.

The Hongchun catchment is an old debris flow gully. Two small debris flows occurred in it historically. One of the debris flows occurred in 1930s, which caused no damages. The other one occurred in August, 1962, in which it rushed out of the gully mouth and partially blocked the Mingjiang River, which caused the water flowed crossing the opposite bank and brought about flood in some area. According to field survey, before the Wenchuan earthquake, around 200×104 m^3 of loose deposits were distributed along both sides of the gully.

The basic data utilized in the study includes a grid digital elevation model (DEM), which was made through the interpolation of contour lines from available topographic map (provided by Sichuan Center of Basic Geographic Information), and a selected aerial photograph taken by Ministry of Land and Resources after the Wenchuan earthquake.

3. Methodology

This paper aims to develop an approach from earthquake-induced landslides investigation to numerical simulation of the debris flow. Therefore, we are especially concerned on 1) identification of the loose deposits of debris flow based on object-oriented analysis; 2) the simulation of the transport process of debris flow based on a two-dimensional numerical model. Because the sediment materials are mostly originated from loose deposits of landslides triggered by the Wenchuan earthquake, landslide detection based on remote sensing technique becomes to the foremost important issue, and then followed by debris flow simulation.

3.1 Landslide identification based on Object-oriented Analysis (OOA)

Generally, landslide can be detected by visual interpretation when images are available. However, visual interpretation is time and labor-consuming especially for a widespread event, and is subject to highly variable degrees of accuracy depending both on the experience of analyst and the scale and quality of the images [16]. Therefore we will detect the landslides semi-automatically by using object-oriented analysis (OOA). Object-oriented image analysis is a knowledge driven method, whereby spectral, morphometric and contextual landslide diagnostic features can be integrated based on expert knowledge to accurately detect landslides [17]. There are two stages involved in OOA for landslide recognition: image segmentation step and image classification step. During the first step, the pixel is combined into ‘regions’, which is with similar properties by taking into account not only spectral information, but also texture, shape and size of the objects. And then these objects are classified based on selected samples or on membership functions allowing users to develop an expert knowledge base in the second step.

(1) Image segmentation

Traditionally, people carry out image classification by pixel-based method, which is ill-suited to represent a geomorphic process such as landslide. Therefore, the 'salt and pepper' phenomenon appeared within the result, and the result is mostly not verifiable on the ground. Instead of single pixels, this paper uses objects to describe the features of interests, which means it needs to create object that is alone or in a group boundary demarcates of the given features. This can be implemented by image segmentation, which is a process of dividing the image into objects or regions based on homogeneity of each pixel value. Image segmentation can be done in different ways, using techniques such as density slicing, split and merge [18].

Landslides pose a particular challenge to image segmentation because they often result in diverse spectral features due to land cover variability or illumination variations. Moreover, in this study, various types and scales of landslides were induced by earthquake and they had different spectral characteristics in the image. Thus, it is impractical to attempt outlining landslides as single segments for only once. Some post-segmentation merging is needed due to typical size and color variability of landslides. Generally, in order to ensure the features of interests are not grouped into segments represented by other features (under-segmentation), and to ensure a feature of interest is not divided into too many small segments (over-segmentation), a smaller scale is preferred to a bigger one, as later merging is possible, while a bigger scale which subsumed the image features into a larger segment cannot be resolved later on. Image segmentation can be carried out in many different ways and our analysis was performed in the feature extraction module of ENVI EX software. The edge-based segmentation algorithm, which is very fast and only requires one input parameter, scale level, was used to obtain a satisfactory segmentation result.

(2) Supervised classification

Once terrain objects are appropriately outlined, a vast number of attributes for each derived object are calculated, such as shape, spectral and texture attributes. The K Nearest Neighbor method was used for image classification. The algorithm considers the Euclidean distance in n-dimensional space of the target to the elements in the training data, where n is defined by the number of object attributions used during classification. This method is generally more robust than traditional nearest-neighbor classifier, since the K nearest distances are used as a majority vote to determine which class the target belongs to. The K Nearest Neighbor method is much less sensitive to outliers and noises in the dataset and generally produces a more accurate classification result compared with traditional nearest-neighbor methods.

In order to classify landslide candidates, it is necessary to assign the training samples. Different landslide type shows different spectral characteristics. As to this case, landslides mainly show three different colors (bright white, shallow cyan and dark gray) (**Fig.3**). Therefore, when selecting the training samples for landslides, we defined them into three categories: a. slide 1; b. slide 2; c. slide 3. Since it is necessary to carry out field survey to define the type of various landslides, we just use different spectral features to divide the different kinds of landslides as shown in **Fig.3**. Finally, the landslides were formed by merging these different kinds of landslide together within ArcGIS. For non-landslide elements, d. forest; e. river; f. shade area and g. the reconstructed Yingxiu Town, which have significant different spectral features from landslides were defined for classification. However, considering the landslides and other residential areas or roads have similar spectral features, we did not define the residential areas or roads category at first in order not to miss the landslide area. Then, the landslides will be recognized as well as some mis-classified areas included.

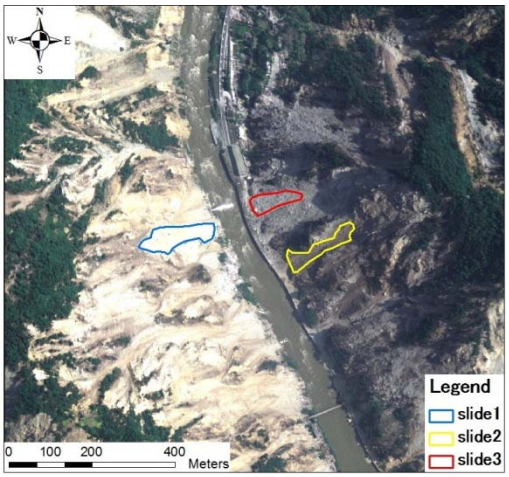

Fig. 3 Three different landslide categories for supervised classification.

(3) Landslide post-processing

Because different terrain features may show the same spectral characteristic, and furthermore, we have not define the residential areas or roads category at first, it is not practical to extract landslides exactly correctly after image classification, some post-processing procedures need to be carried out to improve landslide detection accuracy. In this study, we will integrate DEM derivatives and expert-driven knowledge to produce a better result.

Another limitation of image interpretation need to be paid attention is, the widely used images are two dimensional and they cannot express certain individual landslides. As shown in **Fig.4** (a), several individual landslides are mis-detected as a single one since only 2D information is used. However, when presenting in a 3D scene supported by DEM data, this landslide area is supposed to be consisted of two individual landslides occurred on both sides a valley in fact as shown in **Fig.4** (b). Therefore it is impossible to divide them only by using remote sensing technique. It would give rise to some errors in terms of landslide numbers. Slope unit automatically derived from Arc Hydro tool is proposed to resolve this problem. The detail procedure of slope unit identification is described in Xie et al., 2004 [19].

3.2 Accuracy assessment

Both the number and spatial extent of mapped landslides are considered critical to a subsequent quantitative landslide assessment or disaster relief and rescue works. Therefore, the accuracy of detection results derived semi-automatically from remote sensing data is assessed by comparing the number and spatial extent of extracted landslide inventory with manually prepared one.

When the aim is to detect certain target such as landslide from an image, not to assess the accuracy of the classification results of the whole image, Branching factor, Miss factor, Detection percentage and Quality percentage are effective to express the accuracy of classification result. The four indexes are expressed as the following equations [20].

$$\text{Branching factor (BF)} = \frac{False\ positive}{True\ positive} \tag{1}$$

$$\text{Miss factor (MF)} = \frac{False\ negative}{True\ positive} \tag{2}$$

$$\text{Detection percentage (DP)} = 100 \times \frac{True\ positive}{(True\ positive + False\ negative)} \tag{3}$$

$$\text{Quality percentage (QP)} = 100 \times \frac{True\ positive}{(True\ positive + False\ negative + False\ positive)} \tag{4}$$

Branching and Miss factors, are calculated from mis-recognized (false positive) and unrecognized (false negative), that may be generated during the automatic detection process, indicate two types of potential errors, similar to commission ratio and omission ratio. Detection percentage indicates the landslides correctly recognized (true positive) by the approach. Quality percentage, which is the most stringent measure of accuracy among the above four accuracy estimates, indicates how likely a landslide identified is true [20].

3.3 Debris flow simulation based on a two-dimensional numerical model

3.3.1 Governing equations

Many researchers have proposed mathematical models for debris flow based on the conservation of mass and the momentum of flow. Some of these models are 2D models [21,22]. Depth-averaged method (similar to those in Vreugdenhil's [23]) is used to eliminate explicit dependence on the coordinate normal to the bed. The flow is governed by the following equations:

$$\frac{\partial h}{\partial t} + \frac{\partial M}{\partial x} + \frac{\partial N}{\partial y} = 0 \tag{5}$$

$$\frac{\partial M}{\partial t} + \alpha\frac{\partial (MU)}{\partial x} + \alpha\frac{\partial (MV)}{\partial y} = -\frac{\partial H}{\partial x}gh + v\beta\left(\frac{\partial^2 M}{\partial x^2} + \frac{\partial^2 M}{\partial y^2}\right) - ghcos\theta_x tan\varphi \tag{6}$$

$$\frac{\partial N}{\partial t} + \alpha\frac{\partial (NU)}{\partial x} + \alpha\frac{\partial (NV)}{\partial y} = -\frac{\partial H}{\partial y}gh + v\beta\left(\frac{\partial^2 N}{\partial x^2} + \frac{\partial^2 N}{\partial y^2}\right) - ghcos\theta_y tan\varphi \tag{7}$$

Where $M = Uh$ and $N = Vh$ are the $x-$ and $y-$ components of the flow flux; U and V are the $x-$ and $y-$components of the depth-average velocity; H is height of the free surface; h is flow depth; t is time; θ_x and θ_y are angle of inclination at the bed along the x and y directions, respectively; α is the velocity correction factor; β is the vertical and horizontal normal stress ratio; $v = \mu/\rho_d$ is kinematic viscosity, μ is dynamic viscosity; ρ_d is equivalent density of the debris mixture, and $\rho_d = \rho_s v_s + \rho_w v_w$, ρ_s and ρ_w are densities of solid grains and water, v_s and v_w are volumetric concentrations of solids particles and water in the mixture; and $tan\varphi$ is dynamic friction coefficient.

3.3.2 Numerical simulation

Considering that finite-difference method on rectangular grids is widely used in numerical models for debris flow simulation and the most widely used data structures are grid networks with rows and columns, in which each cell contains a value representing information, such as elevation. Therefore, in this paper, we used grid networks in GIS as the rectangular grids of finite-difference methods since grid-based objects can be easily obtained and managed within GIS.

When carrying out DEM analysis in GIS, each cell has eight possible flow directions (**Fig.5**). The flow direction of a cell is expressed in degrees: left = 0, up = 90, right = 180, down = 270; and the diagonals: 45, 135, 225 and 315. Within a cell, overland flow is routed along one flow direction. The flow direction is the maximum downslope direction, which is determined from the raster-based DEM. The numerical solution using a finite-difference formulation based on the DEM grid was detailed depicted in the previous literature [22].

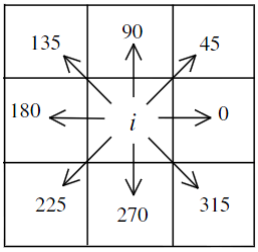

Fig. 5 Possible flow direction in a grid cell.

3.3.3 Simulation of the Hongchun Gully debris flow

Landslides with large scale can be seen as the main loose source material of debris flow. However, the volumetric information of landslide is not available because remote sensing does not reveal 3D information. Thus, field investigation is carried out to define the magnitude of loose deposits. Once the sediment material was determined, the approach proposed above can be used to simulate the Hongchun Gully debris flow.

Since only a 20 m DEM map made before the Wenchuan earthquake is available for generating grids, the area is divided into 200*170 grids by using ArcGIS 9.3. The rheological parameters are assumed as constant throughout the duration of the debris event. According to the previous field investigation result, the bulk density of debris flow in Hongchun Gully is 2.05 g/cm^3 and the sediment concentration C is 62% [4)]. And according to the Detailed Investigation Specification of Landslides, Collapses and Debris Flow in China, when C reached to 40% - 80%, debris flow can be categoried as viscous. Then based on Kang and Zhang (1980) [24)], the viscous debris flow with C is 62%, μ is 11 Pa-s accordingly. So the debris and water mixture is assumed to be a uniform continuous, incompressible, unsteady Newtonian viscous fluid in this study. Furthermore, α is following decided as 1.25 according to Takahashi et al., 1992 [21)], who thought α can be assumed as 1.25 for viscous debris flow. And we assume the vertical normal stress equals to the horizontal normal stress, therefore β =1.00. The detail parameters are shown in **Table 1**.

Table 1 The rheological parameters of the debris flow simulation.

ρ (kg/m^3)	α	β	μ (Pa-s)	g (m/s^2)	$tan\varphi$
2000	1.25	1.00	11	9.8	0.6

4. Results

4.1 Different terrain features classification

Image segmentation is the first step for OOA. Since the natural object size varies from each other, it is impossible to delineate all these objects by using a single segmentation parameter. To ensure the image is rightly segmented, we firstly selected a small scale to avoid under-segmentation, though it leads to a large number of objects. Then, we used a merge level to improve the delineation of feature boundaries based on a very fast edge-based segmentation algorithm. It proves that scale level 30 and merge level 85 were the best segment scale after tests.

Once segments have been divided and different attributes have been calculated, the next procedure is image classification. In order to classify the landslide candidates, training samples need to be assigned. Theoretically, the more features and training samples are selected, the better the results are from supervised classification. However, an overwhelming number of training samples will cause poor performance during classification and previewing classification results. In this study, 30 slide1 (with the bright white color), 20 slide 2 (with the shallow cyan color), 20 slide

3 (with the dark gray color), 15 forest, 3 river, 15 houses in new Yingxiu Town and 15 shade areas are selected as the training samples for supervised classification. **Figure 6** shows the classification result.

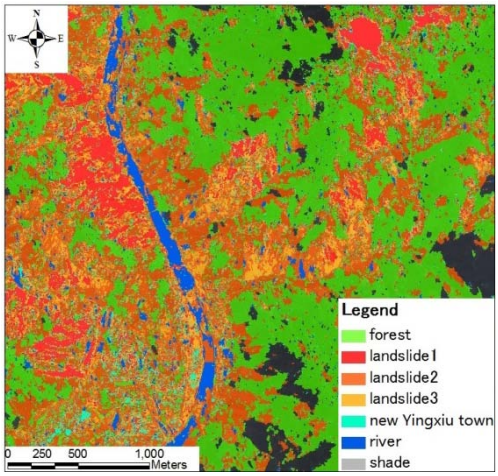

Fig. 6 Different terrain features classification.

From the result showed above, we can see almost all of the landslides were identified, although some misclassified areas were included and some area where landslide3 covered were classified as shade area or forest category. To improve the classification result, non-landslide objects are eliminated by assuming that landslides will not occur for the slope gradient less than 10°. Then some plain areas such as river or residential areas were eliminated. Furthermore, tiny areas less than 20 m^2 were eliminated. The buildings and some crop land were eliminated by rectangularity filtering. **Figure 7** shows the detected earthquake-induced landslides.

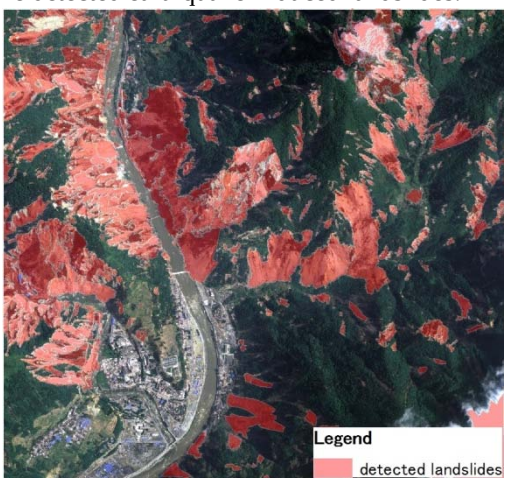

Fig. 7 Semi-automatically detected landslides.

Furthermore, although almost all of area where the landslides occurred is detected (**Fig.9**), several individual landslides are mis-detected as a single one because only 2D information is used. As **Fig.4** shows, in a planner image (**Fig.4** (a)), landslides are supposed to be separated into two slopes (**Fig.4** (b)) with a 3D scene, but they conjoined together in the image, which will lead to statistical error of landslide numbers in the following work. Therefore, we used slope unit to resolve this problem. 331 slope units were divided in total at last. **Figure 4** (c) is an enlarged view of landslides separation result derived by using slope unit.

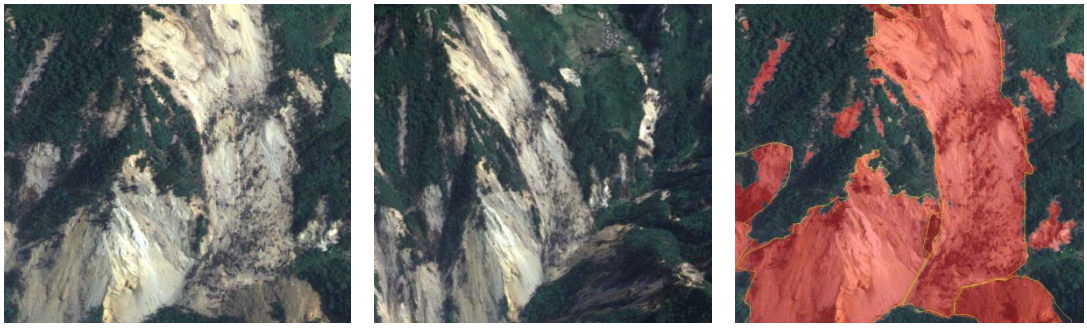

(a) Conjoined landslides showed in the image (b) 3D view of the landslides (c) Landslides division by slope unit

Fig. 4 Separation of conjoined landslides by using slope unit.

4.2 Accuracy assessment of detected landslides

The accuracy of detection results derived semi-automatically based on OOA is assessed by comparing the number and spatial extent of extracted landslide inventory with a manually prepared one. 263 landslides are described in polygon format from a stereoscopic visual interpretation of aerial photograph for preparation of the manually drawn landslide inventory. The results are listed in **Table 2.**

Table 2 Landslide extent comparison based on semi-automatic and manual landslide inventories.

Item	Detected	Manual	Overlapped	BF	MF	DP	QP
Numbers	292	263	215	0.3581	0.2233	0.8175	0.6324
Extent (m^2)	3.384E+06	2.947E+06	2.503E+06	0.3520	0.1773	0.8494	0.6539

According to **Table 2**, we achieve 81.75% and 87.66% overall detection accuracy in terms of landslide numbers and spatial extent in the entire area. It indicates that the boundaries of the landslides are delineated accurately and the outputs can be effectively used for landslide susceptibility mapping by data driven models. Branching factor is 0.3581 and miss factor is 0.2233 for spatial extent, which indicates the omission ratio is relatively low while commission ratio is relatively high.

4.3 Hongchun Gully debris flow simulation

Among the detected landslides in the entire area, 73 landslides are distributed along the Hongchun Gully. Six landslides with large scale shown in **Fig.8**: H1, H2, H3, H4, H5 and H6 were selected as the main source area for forming the loose deposits of the debris flow. Information concerning landslide area was derived from the calculate geometry function within GIS. Because a two-dimensional image view cannot reveal height information of the different features, the volume of each landslide was estimated by field survey. Then the average thickness of each landslide can be obtained through the volume divided by the area. Combing with the field investigation result, the thickness of the deposit layer for each landslide can be assumed as a constant value. The area and average thickness for the above six landslides are shown in **Table 3**. They were uniformly laid in the gully for simulation later.

Table 3 Area and thickness of the selected landslides as loose deposits for Hongchun Gully debris flow.

	H1	H2	H3	H4	H5	H6
Area (km^2)	0.1104	0.0853	0.1167	0.0255	0.0450	0.0603
Average thickness (m)	3	3	5	0.5	1	4

Fig. 8 Identified landslides as loose deposits of the Hongchun Gully debris flow. H is the abbreviations of landslides.

The results from FDM are converted to GIS layers for visualizing. Movements of the debris flow are illustrated in **Fig. 9**(a)-(d) at different time. It can be seen that the river is blocked in **Fig. 9**(d). The distribution of the maximum depth of the whole flow is shown in **Fig.10**. According to the simulation result, the length and width of the debris dam are 483 m and 362 m respectively, while they are 470 m and 350 m respectively according to the field investigation data. The results show that there is a satisfied agreement between the simulation result and field survey data.

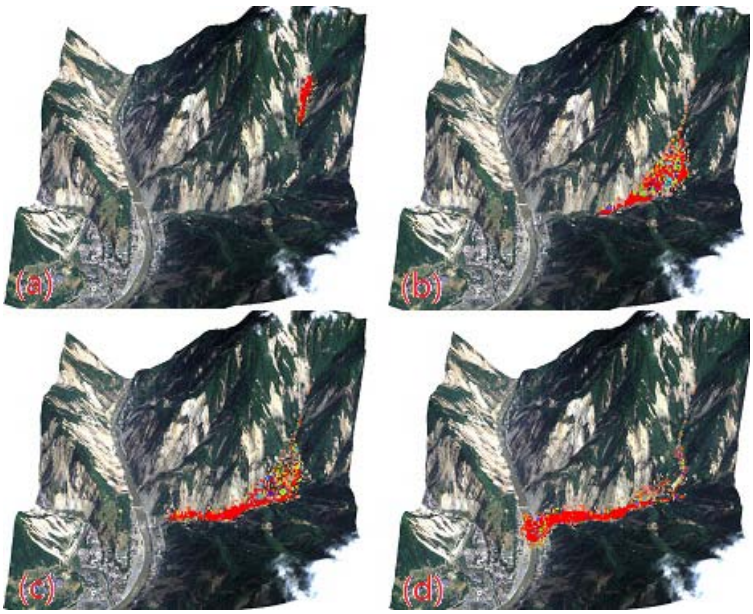

Fig. 9 The movement of the debris flow.

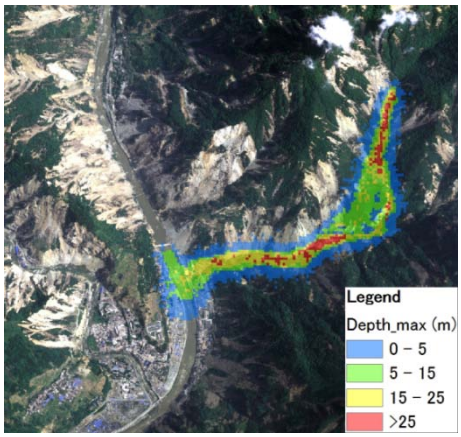

Fig. 10 The distribution of the maximum depth of Hongchun Gully debris flow.

5. Discussions

In this study, we proposed an approach from earthquake-induced landslide identification to numerical simulation of debris flow.

The landslide identification is carried out by image segmentation, image classification and image post-processing. The selection of scales for segmentation of fused image was decided by manually tests and the given scales were case depended. Different terrain features often result in spectrally diverse characteristics, even landslide itself poses a particular challenge to segmentation due to typical size variability or land cover variability like partial vegetation. Thus it is not practical to outline landslides and other objects using one scale. This remains a limitation to our approach. A multi-scale segmentation algorithm is needed for delineating landslide objects. The relatively high error of commission is another limitation, which means we should improve the post-classification procedure based on expert-driven knowledge. We will address these issues in other paper by further study. Further, we extract landslides based on supervised classification, which need define predefined classification types and training samples. Considering the landslides in this area are all fresh, and some naked ground or residential area with similar spectral characteristics, we will take some relatively conservative measures. When we define the classification types, the naked ground and residential area are classified as the landslide type, other than into different types. Only in this way most of landslides can be identified, though some other information will inevitably be contained. This information can be removed by expert-driven knowledge in GIS. For example, we can remove some plain ground by slope gradient and the residential area was deleted by rectangular filter. It turns out that the landslide area can be identified and the omission ratio is acceptable, though commission is still wrongly distinguished. Errors of commission were mainly caused by human-induced terrain disturbance and residential areas confused in classification. We will remove this wrongly identified area by further study.

Although most of landslides areas can be detected, it is worth mentioning that some different landslides are joined into one because two dimensional view of the image cannot express certain individual ones which should belong to two different slopes. Therefore, we use slope unit automatically derived from Arc Hydro tool to resolve this problem. This method can not only respite the conjoint landslides, but also the identified slope units have laid foundation for later landslide related analysis, such as landslide hazard assessment.

The detected large landslides were considered as the loose deposits of the debris flow in

Hongchun Gully, and these landslides were uniformly laid for debris flow simulation. The scope of these may be not the same with the actual accumulation. Moreover, as remote sensing does not reveal 3D information, the landslides volume information is not available. Therefore, we obtained the volume of each landslide deposit by filed investigation. The landslides extent was derived from the geometric calculation function in GIS. Once the extent and volume information is available, the thickness of each landslide can be calculated. The accumulation of deposit thickness is supposed to be a constant value, which is also different from the actual one. Besides, the 2D numerical model that used for debris flow simulation utilized in this paper take the debris flow as one single fluid for simulation, not take the interaction of solid and fluid into account, in this way we cannot calculate the accumulation, corrosion and other characteristics.

6. Conclusions

A strong earthquake not only cause directly damages on construction but also can result in a series of natural disasters such as landslide, debris flow and flooding. These secondary disasters occur as a chain disaster after a catastrophic earthquake. In order to mitigate such kind of risk, apart from engineering measures, we proposed an approach from earthquake-induced landslide identification to numerical simulation of debris flow.

Landslides are identified based on an object-oriented analysis method, which integrates spectral, morphometric and contextual landslide diagnostic features based on expert knowledge to accurately detect landslides. Through comparing the numbers and spatial extent of semi-automatically detected landslides with a manually prepared landslide inventory map, we achieved 81.75% and 87.66% detection accuracy respectively in terms of landslide numbers and extent in the entire area.

The image interpretation gave us a good understanding into the sediment deposits of debris flow. A depth-averaged 2D numerical model incorporating the grid in ArcGIS used as the finite difference mesh was used to simulate the debris flow in Hongchun Gully. The simulation can show us a real propagation process of the debris flow, the potential inundation area can be derived and the maximum depth in the flow gully was calculated.

Acknowledgements

This study has received financial support from Grants-in-Aid for Scientific Research (Scientific Research (B), 22310113, G. Chen) from Japan Society for the Promotion of Science and the Research Fund of the State Key Laboratory of Geo-Hazard Prevention of China (SKLGP2009Z004). The financial supports are gratefully acknowledged.

References

1) Xu, Q., Zhang, S., Li, W.L.; “Spatial Distribution of Large-scale Landslides Induced by the 5.12 Wenchuan Earthquake”. Science Press and Institute of Mountain Hazards and Environment, J. Mt. Sci. Vol.8, pp.246-260. DOI: 10.1007/s11629-011-2105-8 (2011).
2) Dai, F., Xu, C., Yao, X., Xu, L., Tu, X., Gong, Q.; “Spatial distribution of landslides triggered by the 2008 Ms 8.0 Wenchuan earthquake, China”. Journal of Asian Earth Sciences, Vol. 40, No. 4, pp. 883-895 (2011).
3) Lin, C.W., Liu, S.H., Lee, S.Y., Liu, C.C.; “Impacts of the Chi-Chi earthquake on subsequent rain-induced landslides in central Taiwan”. Engineering Geology, Vol.86, pp.87-101 (2006).
4) Tang, C., Zhu, J., Qi, X., Ding, J.; “Landslides induced by the Wenchuan earthquake and the

subsequent strong rainfall event: A case study in the Beichuan area of China". Engineering Geology, doi:10.1016/j.enggeo.2011.03.013, ISSN 0013-7952 (2011).

5) Takahashi, T.; "Estimation of potential debris flows and their hazardous zones". J Nat Disaster Sci, Vol.3, pp.57-89 (1981).
6) Nichol, J., Wong, M.S.; "Satellite remote sensing for detailed landslide inventories using change detection and image fusion". International Journal of Remote Sensing, Vol.26, pp.1913-26 (2005a).
7) Cheng, K.S., Wei, C. and Chang, S.C.; "Locating landslides using multi-temporal satellite images". Advances in Space Research, Vol.33, pp. 296-301 (2004).
8) Mondini, A.C., Chang, K.T., Yin, H.Y.; "Combining multiple change detection indices for mapping landslides triggered by typhoons". Geomorphology, Vol.134, pp.440-451 (2011).
9) Borghuis, A.M., Chang, K., Lee, H.Y.; "Comparison between automated and manual mapping of typhoon-triggered landslides from SPOT-5 imagery". International Journal of Remote Sensing, Vol.28, pp.1843-1856 (2007).
10) Nichol, J., Wong, M.S.; "Detection and interpretation of landslides using satellite images". Land Degradation and Development, Vo.16, pp. 243-55 (2005b).
11) Barlow, J., Franklin, S., Martin, Y.; "High spatial resolution satellite imagery, DEM derivatives, and image segmentation for the detection of mass wasting processes". Photogrammetric Engineering and Remote Sensing, Vol.72, pp.687-692 (2006).
12) Martha, T.R., Kerle, N., Jetten, V., van Westen, C.J., Kumar, K.V.; "Characterising spectral, spatial and morphometric properties of landslides for semi-automatic detection using object-oriented methods". Geomorphology, Vol. 116, pp. 24-36 (2010).
13) Takahashi, T.; "Mechanical characteristics of debris flow". J. Hydraulic Div., ASCE 104(HY8). pp.1153-1169 (1978).
14) Coe, J.A, Kinner, D.A, Godt, J.W. "Initiation conditions for debris flows generated by runoff at Chalk Cliffs, central Colorado". Geomorphology, Vol. 96 (3-4), pp. 270-297 (2008).
15) Glade, T.; "Linking debris-flow hazard assessments with geomorphology". Geomorphology, Vol.66, pp.189-213 (2005).
16) Brardinoni, F., Slaymaker, O., Hassan, M.; "Landslide inventory in a rugged forested watershed: A comparison between air photo and field survey data". Geomorphology, Vol.54, pp.179-196 (2002).
17) Barlow, J., Martin, Y., Franklin, S.E.; "Detecting translational landslide scars using segmentation of Landsat ETM+ and DEM data in the northern Cascade Mountains, British Columbia". Canadian Journal of Remote Sensing, Vol.29, pp.510-517 (2003).
18) Kerle, N., de Leeuw, J.; "Reviving legacy population maps with object-oriented image processing techniques". IEEE Transactions on Geoscience and Remote Sensing, Vol.47, pp.2392-2402 (2009).
19) Xie, M.W., Esaki, T. and Zhou, G.Y.: GIS-Based Probabilistic Mapping of Landslide Hazard Using a Three-Dimensional Deterministic Model, Natural Hazards 33: 265-282, 2004.
20) Lee, D.S., Shan, J., Bethel, J.S.; "Class-guided building extraction from Ikonos imagery". Photogrammetric Engineering and Remote Sensing, Vol.69 (2), pp.143-150 (2003).
21) Takahashi, T., Nakagawa, H., Harda, T., Yamashiki, Y.; "Routing debris flows with particle segregation". Hydraulic Eng, Vol.118, pp.1490-1507 (1992).
22) Wang, C.X., Tetsuro, E., Xie, M.W., Qiu, C.; "Landslide and debris-flow hazard analysis and prediction using GIS in Minamata-Hougawachi area, Japan". Environmental Geology, Vol.51, Issue 1, pp.91-102 (2006).
23) Vreugdenhil, C.B.; "Numerical methods for shallow-water flow". Kluwer Academic Publishers,

Norwell, (1994).

24) Kang, Z., Zhang, S.; “A preliminary analysis of the characteristics of debris flow”. Proceedings of the International Symposium on River Sedimentation. Chinese Society for Hydraulic Engineering, Beijing, pp.225-226 (1980).